

# Langmuir Film-Forming and Second Harmonic Generation Properties of Lanthanide Complexes

Chunhui Huang,\* Kezhi Wang, and Guangxian Xu

State Key Laboratory of Rare Earth Materials Chemistry and Applications, Peking University, Beijing 100871, China

Xinsheng Zhao and Xiaoming Xie

College of Chemistry and Molecular Engineering, Peking University, Beijing 100871, China

Yu Xu and Yunqi Liu

Institute of Chemistry, Academia Sinica, Beijing 100080, China

Linge Xu and Tiankai Li

Institute of Photographic Chemistry, Academia Sinica, Beijing 100101, China

Received: September 30, 1994; In Final Form: June 5, 1995<sup>⊗</sup>

A series of amphiphilic lanthanide complexes were designed and synthesized, in which the lanthanide complex anions act both as the counterions of hemicyanine and as the spacer within a Langmuir–Blodgett (LB) film. Studies on the surface pressure–area ( $\pi$ – $A$ ) isotherms of these complexes show that the film-forming properties can be clearly improved if appropriate  $\beta$ -diketone ligands were chosen. The effects of molecular structures of the complexes, including the variation of lanthanide central ions, the structures of  $\beta$ -diketone ligands, and the length of alkyl chains in hemicyanines, on the film-forming properties of the materials are discussed. From second-harmonic generation experiments, the largely enhanced second-order molecular hyperpolarizability of lanthanide complexes with good film-forming properties were obtained compared with the hemicyanine iodide. This effect may be due in part to the local field effect but primarily molecular ordering and ordered segregation of hemicyanine chromophores by the bulky lanthanide complex anions. The charge separation of the hemicyanine chromophores was supported by the crystal structure of a model complex. The homogeneity of the film was verified by low angle X-ray diffraction and also by the linear relationship of the absorbance vs the number of layers of the LB films of a selected complex.

## Introduction

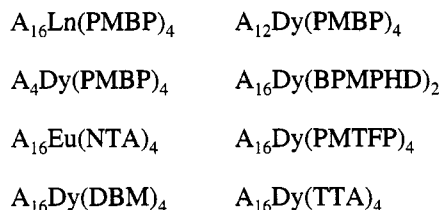
Much interest has been paid to organic second-order nonlinear optical materials<sup>1,2</sup> due to their much higher nonlinear efficiencies than currently available inorganics,<sup>3,4</sup> high resistance to laser-induced damage, and potential applications in various areas of optoelectronics including optical communication, electrooptical device and laser scanning.<sup>5</sup> Unfortunately, some of the promising compounds with high microscopic polarizability crystallize in a centrosymmetric environment, thus canceling these tensors, leading to materials with vanishing bulk polarizability  $\chi^{(2)}$ .<sup>6</sup> The Langmuir–Blodgett (LB) technique can overcome this difficulty by aligning suitable chromophores in a noncentrosymmetric array and allowing the tailoring of the bulk nonlinear medium. In addition, in consideration of mode confinement in integrated optics, LB film deposition provides precisely controlled film thickness. The monolayer and LB films of amphiphilic derivatives of the (dimethylamino)-stilbazolium chromophores (hemicyanines) have been extensively investigated.<sup>7–10</sup> Film forming and second harmonic generation (SHG) properties of these films showed strong counteranion dependence and sensitivity to the extent of molecular aggregations.<sup>7–9</sup> In some cases, dye molecules had to be mixed with an inert phase,<sup>8–10</sup> such as stearic acid, to improve the film-forming properties and reduce inferior H aggregation, but this has the potential disadvantage of phase

separation. Very recently, using lanthanide complexes as the counter ions of second-order nonlinear active chromophores, we improved the film-forming and second harmonic generation properties of the materials without the danger of the phase separation.<sup>11</sup> To best understand this phenomena, it is imperative that systematic work on a series of lanthanide complexes with different molecular structures be carried out. Also, the functionality of lanthanide ions or their metal complexes, such as magnetism,<sup>12–15</sup> may be introduced into the LB films.

## Experimental Section

**Chemicals.** (*E*)-*N*-*n*-Alkyl-4-(2-(4-(dimethylamino)phenyl)-ethenyl)pyridinium bromide ( $n = 16, 12, 4$  and abbreviated A<sub>16</sub>-Br, A<sub>12</sub>-Br, A<sub>4</sub>-Br, respectively) and corresponding iodide A<sub>16</sub>I,<sup>16</sup>  $\beta$ -naphthoyltrifluoroacetone (HNNTA),<sup>17</sup> 1,6-bis(1'-phenyl-3'-methyl-5'-pyrazolone-4')hexanedione[1,5] (H<sub>2</sub>BPMPHD),<sup>18</sup> and 1-phenyl-3-methyl-4-(trifluoroacetyl)-5-pyrazolone (HPMTFP)<sup>19</sup> were prepared according to the literature methods, respectively. Aqueous lanthanide (La, Nd, Dy, and Yb) nitrate (ca. 1 mol/L) were obtained by dissolving corresponding Ln<sub>2</sub>O<sub>3</sub> in slightly excessive nitric acid. 1-Phenyl-3-methyl-4-benzoyl-5-pyrazolone (HPMBP),  $\alpha$ -thenoyltrifluoroacetone (HTTA), dibenzoylmethane (HDBM) are of A. R. grade and commercially available. Eleven lanthanide  $\beta$ -diketonate or bis- $\beta$ -diketonate complexes with following compositions were synthesized in a similar manner:

<sup>⊗</sup> Abstract published in *Advance ACS Abstracts*, September 1, 1995.



in which  $A_n = Me_2NC_6H_4CH=CHC_5H_4NC_nH_{2n+1}$  ( $n = 16, 12, 4$ ). The general synthetic procedures of the metal complexes are as follows.

To an aqueous ethanol solution of stoichiometric molar ratios of  $A_nBr$  and  $\beta$ -diketone or bis- $\beta$ -diketone ligands neutralized with aqueous NaOH solution was added dropwise stoichiometric aqueous  $Ln(NO_3)_3$  ( $Ln = La, Nd, Dy, \text{ and } Yb$ ) under vigorous stirring. The resulting mixture was refluxed half an hour in a water bath. Isolated precipitate was filtered out and purified by recrystallization from suitable solvent. Anal. Calcd for  $A_{16}La(PMBP)_4(C_{99}H_{101}N_{10}O_8La)$ : C, 70.03; H, 6.00; N, 8.25; La, 8.19. Found: C, 69.86; H, 6.20; N, 7.88; La, 8.00. Mp 62 °C. Anal. Calcd for  $A_{16}Nd(PMBP)_4(C_{99}H_{101}N_{10}O_8Nd)$ : C, 69.82; H, 5.98; N, 8.22; Nd, 8.19. Found: C, 70.00; H, 6.04; N, 8.03; Nd, 8.00. Mp 66.7 °C. Anal. Calcd for  $A_{16}Dy(PMBP)_4(C_{99}H_{101}N_{10}O_8Dy)$ : C, 69.08; H, 5.91; N, 8.13; Dy, 9.44. Found: C, 69.10; H, 5.78; N, 8.14; Dy, 9.27. Mp 65.4 °C. Anal. Calcd for  $A_{16}Yb(PMBP)_4(C_{99}H_{101}N_{10}O_8Yb)$ : C, 69.67; H, 5.88; N, 8.08; Yb, 9.99. Found: C, 69.32; H, 5.72; N, 8.15; Yb, 10.03. Mp 67.0 °C. Anal. Calcd for  $A_{12}Dy(PMBP)_4(C_{95}H_{93}N_{10}O_8Dy)$ : C, 68.53; H, 5.59; N, 8.40; Dy, 9.77. Found: C, 68.84; H, 5.73; N, 8.42; Dy, 9.89. Mp 198 °C. Anal. Calcd for  $A_4Dy(PMBP)_4(C_{87}H_{77}N_{10}O_8Dy)$ : C, 66.95; H, 4.79; N, 9.19; Dy, 10.50. Found: C, 66.78; H, 4.77; N, 9.15; Dy, 10.70. Mp 272 °C. Anal. Calcd for  $A_{16}Dy(BPMPHD)_2(C_{83}H_{93}N_{10}O_8Dy)$ : C, 65.10; H, 6.36; N, 9.19; Dy, 10.67. Found: C, 64.60; H, 6.36; N, 9.25; Dy, 10.51. Mp 290 °C (dec). Anal. Calcd for  $A_{16}Eu(NTA)_4(C_{87}H_{81}F_{12}N_2O_8Eu)$ : C, 62.84; H, 4.91; N, 1.68. Found: C, 62.81; H, 4.86; N, 1.54. Mp 145 °C. Anal. Calcd for  $A_{16}Dy(DBM)_4(C_{91}H_{93}N_2O_8Dy)$ : C, 72.65; H, 6.38; N, 1.86; Dy, 10.80. Found: C, 72.33; H, 6.45; N, 2.01; Dy, 10.49. Mp 215 °C (dec). Anal. Calcd for  $A_{16}Dy(PMTFP)_4(C_{79}H_{81}F_{12}N_{10}O_8Dy)$ : C, 56.2; H, 4.80; N, 8.29; Dy, 9.63. Found: C, 55.61; H, 4.57; N, 8.23; Dy, 9.80. Mp 178 °C. Anal. Calcd for  $A_{16}Eu(TTA)_4(C_{63}H_{65}F_{12}N_2O_8S_4Eu)$ : C, 50.93; H, 4.38; N, 1.89; Eu, 10.40. Found: C, 50.00; H, 4.30; N, 1.65; Eu, 10.40. Mp 132 °C.

**Film Preparation.** The LB films were prepared with a British Joyce-Loebl model computer-controlled LB trough. A given amount of the metal complexes were dissolved ultrasonically in  $C_6H_6$  or freshly distilled  $CHCl_3$  (concentration ranging from  $0.67 \times 10^{-3}$  to  $1.67 \times 10^{-3}$  mol/L). The solutions of the complexes were spread on a pure water subphase (18 °C, pH 5.6). After complete evaporation of the solvent, the surface pressure-area isotherms were recorded at a speed of 22  $cm^2/min$ . At a constant surface pressure (12 mN/m for  $A_{16}Ln(PMBP)_4$ ,  $Ln = La, Nd, Dy, \text{ and } Yb$ ; 15 mN/m for  $A_{12}Dy(PMBP)_4$ ; 25 mN/m for  $A_{16}Dy(BPMPHD)_2$ ; 10 mN/m for  $A_4Dy(PMBP)_4$ ; 25 mN/m for  $A_{16}Eu(NTA)_4$ ; 20 mN/m for  $A_{16}Dy(PMTFP)_4$ ; 20 mN/m for  $A_{16}Eu(TTA)_4$  and  $A_{16}Dy(DBM)_4$ ), the floating films were transferred onto the hydrophilically pretreated substrates by the vertical dipping (VD) method with a dipping speed of 5 mm/min. The deposition occurred upon upstroke, so the multilayer films are known as Z-type structure. Just prior to film deposition, hydrophilic treatment of substrates, either quartz, single crystal  $CaF_2$ , or optical glass, was completed by being washed first with degreased detergent and then

deionized water, ethanol, and chloroform in an ultrasonic bath for 30 min each and finally dried in a jet of dry dinitrogen.

**Measurements and Instruments.** UV-vis spectra were obtained on a Shimadzu UV-240 spectrophotometer. IR spectra were measured on a Nicolet 7199B FT-IR system. X-ray diffractograms were obtained on a Rigaku D/max-3B diffractometer with a  $Cu K\alpha$  radiation of a wavelength of 0.154 nm. Second harmonic generation (SHG) experiments were carried out in transmission with a Nd:YAG 1 064  $\mu m$  laser as incident fundamental light. The setup of SHG was similar to that used in literature<sup>20</sup> except for additional 0.532  $\mu m$  passed monochromator. Prior to the SHG measurements, the films at the back sides of the substrates were wiped off carefully with lens tissues soaked in chloroform in order to prevent interference between signals arising from the monolayers at the front and backside of the substrate.

### Method of Data Treatment

The data of second-harmonic generation (SHG) from the LB films were analyzed by the general procedure described by Ashwell et al.<sup>7</sup> However, the method differs from that of Zhang et al.,<sup>21</sup> which is restricted to the reflection experiments of the SHG. On assumption that the chromophores have a common tilt angle  $\phi$  with respect to the normal of the film surface, with a random azimuthal distribution, and that the second-order molecular hyperpolarizability ( $\beta$ ) is dominated by the component along the intramolecular donor- $\pi$ -acceptor axis, the following simplified equations can be obtained:

$$\frac{I_{2\omega}(p \rightarrow p)}{I_{2\omega}(s \rightarrow p)} = \frac{(\chi^{(2)}(zzz)\sin^3 \theta + 3\chi^{(2)}(zxx)\sin \theta \cos^2 \theta)^2}{(\chi^{(2)}(zxx)\sin \theta)^2} \quad (1)$$

$$\chi^{(2)}(zzz) = \chi^{(2)} \cos^3 \phi = N f_{2\omega}(f_{\omega})^2 \beta \cos^3 \phi \quad (2)$$

$$\chi^{(2)}(zxx) = 0.5\chi^{(2)} \cos \theta \sin^2 \phi = 0.5N f_{2\omega}(f_{\omega})^2 \beta \cos \phi \sin^2 \phi \quad (3)$$

in which  $\theta = 45^\circ$  is the angle of laser beam to the film;  $I_{2\omega}(p \rightarrow p)$  is the p-polarized double-frequency signal intensity with p-polarized incidental fundamental light;  $I_{2\omega}(s \rightarrow p)$  is p-polarized double-frequency signal intensity with s-polarized incidental fundamental light;  $N$  is the number of molecules per unit volume;  $f_{\omega,2\omega} = [(n_{\omega,2\omega} + 2)]/3$  is a local field correction factor, where  $n_{\omega}$  and  $n_{2\omega}$  are the refractive indexes of the film at fundamental and second-harmonic frequencies, respectively, and the  $n_{2\omega}$  is usually slightly higher than the  $n_{\omega}$ .<sup>22</sup> But in this treatment,  $n$  is taken to be  $n_{\omega} \approx n_{2\omega} = 1.7$ .<sup>7</sup> It means that the changes in local field effect were neglected when the iodide ion in  $A_{16}I$  was replaced by the lanthanide complex anions. It was reported that microscopic local field effect is sensitive to tilt angle  $\phi$  at high surface densities.<sup>23,24</sup> The effect of above approximate treatment ( $n_{\omega} \approx n_{2\omega} = 1.7$ ) dealing with local field on thus derived  $\beta$  values will be discussed in the part of results and discussion.

The combination of eqs 1–3 gives the eq 4, from which the  $\phi$  angle can be derived:

$$\tan(\phi) = [(I_{2\omega}(p \rightarrow p)/I_{2\omega}(s \rightarrow p))^{1/2} - 3/2]^{-1/2} \quad (4)$$

In SHG experiments, by the comparison of polarization dependent SH intensities from monolayer films of the complexes with the signal from Y-cut quartz reference ( $d_{11}$ , 0.5 pm/V),

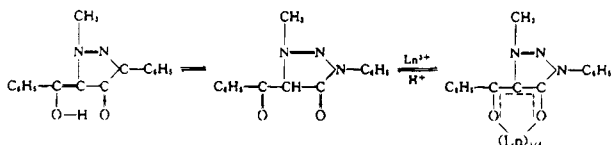
the susceptibility  $\chi^{(2)}$  can be obtained. Then the values of  $\beta$  were calculated based on eq 3.

## Results and Discussion

**Characterization of the Metal Complexes.** As stated above, this series of metal complexes can be easily prepared and purified. The result of elementary analysis listed above are consistent with the composition of 1:1 ion-dissociation type complexes  $A_nLn(L)_i$  (where  $n = 16, 12,$  and  $4, i = 4$  or  $2$  for  $L = \text{BMPHMD}$ ). The complexes were well characterized by UV-vis, IR,  $^1\text{H NMR}$ , X-ray photoelectron spectroscopy (XPS), X-ray powder diffraction, and molar conductivity. The characterization of the complexes  $A_{16}Ln(\text{PMBP})_4$  ( $Ln = \text{La, Nd, Dy, and Yb}$ ) is exemplified as follows:

For the visible spectra of the complexes in  $\text{CHCl}_3$ , each of them exhibits one peak at ca. 490 nm due to charge transfer of hemicyanine cation, which blue-shifts 6 nm compared with that of  $A_{16}\text{I}$ . In the case of Nd complex, two sharp peaks of nonhypersensitive transition  $^4\text{I}_{9/2} \rightarrow ^4\text{F}_{9/2}^{25}$  occurs at 739 and 754 nm, respectively, while two peaks of hypersensitive transition  $^9/2\text{I}_{9/2} \rightarrow ^2\text{G}_{7/2} + ^4\text{G}_{5/2}$  centered at ca. 570 and 580 nm are obscured by the absorption of hemicyanine cation. The ultraviolet spectra of the complexes are very similar, exhibiting two peaks, which is characteristic absorption of ligand HPMBP. The peak at ca. 248 nm for HPMBP is subjected to a blue shift of 8 nm upon ligation and is usually assigned to  $\pi \rightarrow \pi^*$  transition on carbonyl group, coordination of carbonyl oxygen to rare earth ion result in large peak shift; while the peak at 280 nm of HPMBP which corresponds to  $\pi \rightarrow \pi^*$  transition of aromatic ring, remains unchanged.

The IR spectrum for free HPMBP exhibits peaks of  $\text{N}=\text{C}=\text{O}$  at 1646 and  $1600\text{ cm}^{-1}$ , respectively,  $\Delta\nu = 46\text{ cm}^{-1}$ . The former shifts to low wavenumber, while the latter to high wavenumber in the spectra of the complexes. For the La complex, the two peaks shift to 1577.3 and  $1610.9\text{ cm}^{-1}$ ,  $\Delta\nu = 33.6\text{ cm}^{-1}$ ; for Nd complex, to 1577.7 and  $1611.8\text{ cm}^{-1}$ ,  $\Delta\nu = 34.1\text{ cm}^{-1}$ ; for Dy complex, to the 1578.7 and  $1615.0\text{ cm}^{-1}$ ,  $\Delta\nu = 36.3\text{ cm}^{-1}$ ; for Yb complex, to the 1579.1 and  $1618\text{ cm}^{-1}$ ,  $\Delta\nu = 39.8\text{ cm}^{-1}$ . The former peak is assigned to  $\nu_{\text{C}=\text{O}}$  vibration at 5-position of pyrazolone ring. The coordination of lanthanide ions to oxygen of the carbonyl weaken the  $\text{C}=\text{O}$  bond, result in a red shift. While the latter is assigned to  $\nu_{\text{C}=\text{O}}$  vibration of benzoyl in 4-position of pyrazolone ring. This  $\text{C}=\text{O}$  bond has single bond characteristic due to keto-enol tautomer of diketone and was intensified by equalization of single-double bond length upon ligation. Therefore it gave a blue-shift of  $\nu_{\text{C}=\text{O}}$  vibration, this process can be diagrammatically described as follows:



X-ray photoelectron spectroscopy for Dy complex shows peaks at ca. 155.8, 284.8, 399.9, and 531.1 eV which correspond to characteristic peaks of  $\text{Dy}4d_{2/5}$ , C1s, O2p and N1s, respectively. On the basis of the peak strengths and sensitivity factors, calculated ratio of atomic numbers C:O:N is 10.1:0.89:1, which agrees well with theoretical ratio of 9.9:0.8:1.

$^1\text{H NMR}$  spectrum of HPMBP shows a sharp singlet at +2.00 ppm, it is assigned to three methyl proton of the free ligand based on the position and integrated intensity of the signal, a multiplet (6.24–7.95 ppm) ascribed to the 10 phenyl protons, and a small broad peak at intensity of 11.8 ppm which disappears

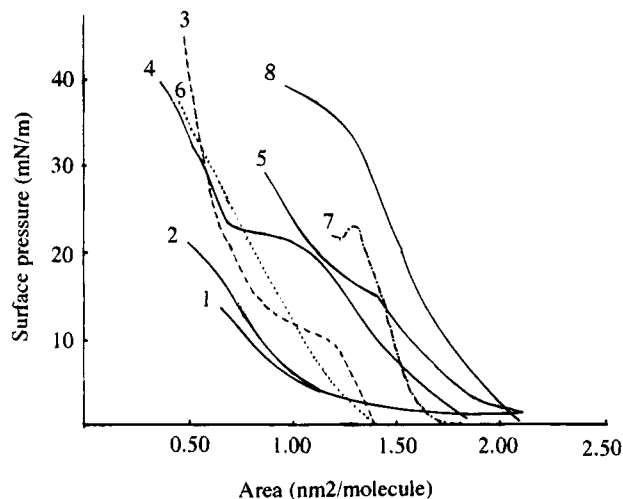


**Figure 1.** Influence of structures of ligands on the film-forming properties: (1)  $A_{16}\text{Br}$ ; (2)  $A_{16}\text{I}$ ; (3)  $A_{16}\text{Dy}(\text{NTA})_4$ ; (4)  $A_{16}\text{Dy}(\text{TTA})_4$ ; (5)  $A_{16}\text{Dy}(\text{PMTFP})_4$ ; (6)  $A_{16}\text{Dy}(\text{DBM})_4$ ; (7)  $A_{16}\text{Dy}(\text{PMBP})_4$ ; (8)  $A_{16}\text{Dy}(\text{BMPHMD})_2$ .

on exchange with  $\text{D}_2\text{O}$ , is attributable to a hydroxyl proton, indicating that the ligand exists as an enol in  $\text{CDCl}_3$ . In the complex, the signal of the hydroxy proton disappears, indicating the coordination reaction has taken place and hydrogen dissociated off, and methyl multiplet shifts to upfield at 1.54 ppm, which is common in the lanthanide complexes of HPMBP and may be due to contact and pseudoconstant interactions.<sup>26</sup> In addition, both proton peaks at 3.06 ppm for dimethylamino group in hemicyanine and at 0.87–1.24 ppm for alkyl chain basically remain unchanged. The molar conductivities of the complexes in nitromethane solution (ca.  $10^{-3}\text{ mol/L}$ ) were found to be around  $65\text{--}75\text{ S mol}^{-1}\text{ cm}^2$ , showing that the complexes are 1:1 ion-dissociation type ones.<sup>27</sup>

**Effect of Ligand Structures in Complex Anions on Film-Forming Properties and Second-Harmonic Generation (SHG) from Monolayer Films.** The surface pressure–area ( $\pi$ – $A$ ) isotherms on pure water subphase (18 °C, pH 5.6) for a series of complexes with the compositions of  $\text{Me}_2\text{NC}_6\text{H}_4\text{CH}=\text{CHC}_3\text{H}_4\text{NC}_{16}\text{H}_{33}\text{Dy}(\text{L})_j$  ( $j = 4$ , except for  $\text{BMPHMD } j = 2$ ), and corresponding hemicyanine bromide and iodide are shown in Figure 1. From the curves, we can obtain the collapse pressures and slopes in condensed regions of  $\pi$ – $A$  curves and the molecular areas by the extrapolation of the condensed regions to surface pressure  $\pi = 0$ . Generally speaking, the larger the collapse pressures and slopes in condensed regions, the better the film-forming properties of the complexes. Collapse pressures, the slopes in condensed region of the complexes are given in Table 1. In the metal complexes mentioned above, the hemicyanine counterion and central ion remain unchanged; only the ligands  $L$  were varied. Hemicyanine bromide and iodide are slightly water soluble, so exhibiting low collapse pressures of 15.0, 20.5 mN/m and condensed region slopes of 0.30 and 0.40, respectively, i.e., both hemicyanine bromide and iodide have poor film-forming properties, but it is obvious from Figure 1 that steeper condensed regions and larger collapse pressures for the complexes than that for hemicyanine bromide and iodide can be obtained, especially for  $L = \text{NTA, BMPHMD, or PMBP}$ . The film-forming properties of materials were obviously improved to some extent if the bromide or iodide counterion of hemicyanine was replaced by lanthanide complex anions.  $\beta$  values in Table 1 are strongly anion dependent and enhanced as the bromide or iodide counterions of hemicyanine were replaced by lanthanide complex anions. But markedly enhanced  $\beta$  values compared with hemicyanine iodide are obtained only

**TABLE 1: Influence of the Ligand Structures of in  $A_{16}X$  on the Film-Forming Properties and SHG**

materials	slope in condense region	collapse pressure (mN/m)	molecular area (nm <sup>2</sup> )	$\chi^{(2)} \times 10^6$ (esu)	$\beta \times 10^{28}$ (esu)	$\phi$ (deg)	ref
$A_{16}Dy(PMBP)_4$	1.08	24.7	1.34	0.59–0.87	6.6–9.3	26.1	this work
$A_{16}Dy(BPMPHD)_2$	0.94	39.4	1.84	0.75–1.20	10.0–15.6	48.9	this work
$A_{16}Dy(PMTFP)_4$	0.50	29.4	1.47	0.40–0.58	4.2–6.2	33.5	this work
$A_{16}Dy(DBM)_4$	0.49	37.8	1.18	0.24–0.34	2.0–3.2	45.4	this work
$A_{16}Dy(TTA)_4$	0.49	38.0	1.09	0.49–0.73	3.8–5.6	37.5	this work
$A_{16}Eu(NTA)_4$	1.20	45.0	0.80	1.0–1.4	6.0–9.0	63.0	this work
$A_{16}I$	0.4	20.5	1.07	0.35–0.50	2.4–3.6	41.1	this work
$A_{18}Br$				0.55–0.85	1.2–1.6	40.0	7
$A_{18}I$				0.55–0.85	1.7–2.7	41.0	7
$A_{22}Br$				0.95	2.3	43.0	28, 29

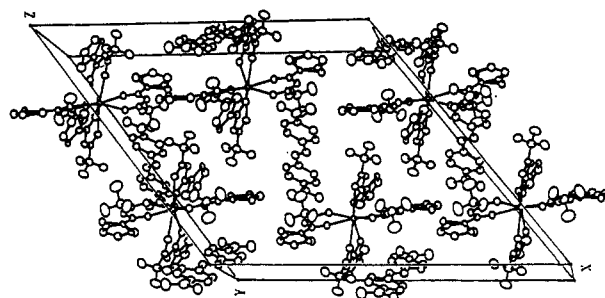
for the complexes with larger slopes in the condensed regions, while the increase of collapse pressure seems to have no benefit for  $\beta$  values.

A number of groups have observed the decrease of second-harmonic intensity at high surface intensities. Some have attributed this decrease to centrosymmetric structure of the aggregate,<sup>30,31</sup> to the blue shift of the spectra which leads to a decrease of the resonance enhancement<sup>32</sup> or to the combination of both of them.<sup>8</sup> Others have ascribed this decrease to a combination of aggregation and the classical microscopic local field effect.<sup>23,24,33–35</sup>

According to Schildkraut et al.,<sup>8</sup> SHG intensities are sensitive to the extent of molecular aggregations, which can be restrained by diluting the chromophore layer with an inert phase such as behenic acid, a 1:1 film of the hemicyanine and behenic acid exhibits a large bathochromic shift of the absorption band from 439 to 477 nm and 44-fold increase in SHG intensity, this is due in part to resonance enhancement. However, except for the monolayer film of  $A_{16}Eu(NTA)_4$  which has comparatively strong absorption at the double frequency of 532 nm due to its small molecular area, the monolayers of all other lanthanide complexes we studied have nearly same spectral overlap at a double frequent wavelength of 532 nm as that of hemicyanine iodide. As a result, the enhanced SH signals in our systems are not responsible for the change in the concentrations of aggregations and resonant enhancement.

According to Cnossen et al.,<sup>23,24</sup> when local field corrections are not being made, the values of  $\beta$  deduced from experiments at high surface density can be grossly overestimated for very high tilt angles or underestimated for very low angles. Usually as high as 3 times overestimation or underestimation can be anticipated. However, it should be pointed out that at low surface densities the local field effect is insensitive to the changes in the tilt angles of chromophore. As can be seen from Table 1, for the film-forming materials we studied, the surface densities vary range from  $0.54 \times 10^{14} \text{ cm}^{-2}$  for  $A_{16}Dy(BPMPHD)_2$  to  $1.25 \times 10^{14} \text{ cm}^{-2}$  for  $A_{16}Eu(NTA)_4$ , which lie not among so called "high surface density region" mentioned by Cnossen et al.<sup>23,24</sup> but among the surface density region in which the local field effect is insensitive to the changes in tilt angles (26.1–63.0° for the systems in this paper). This can be clearly seen in Figure 2 provided by ref 23 or 24, respectively. In particular, the tilt angle of chromophores in the film of complex  $A_{16}Dy(PMBP)_4$  is smaller than that of hemicyanine iodine  $A_{16}I$  and that of  $A_{16}Dy(BPMPHD)_2$  is comparable. Namely, although the changes in local field effect do exist in the nonlinear optical systems we studied, the changes cannot make a dominant contribution to the appreciable enlargements in  $\beta$  values for the complexes  $A_{16}Dy(PMBP)_4$ ,  $A_{16}Dy(BPMPHD)_2$ , and  $A_{16}Dy(NTA)_4$ .

According to Ashwell et al.,<sup>7</sup> SHG signals were appreciably improved when the counter bromide or iodide ions were replaced by octadecylsulfate anion without the changes in visible spectra.

**Figure 2.** Packing diagrams of the complex  $A_2La(TTA)_4$ .

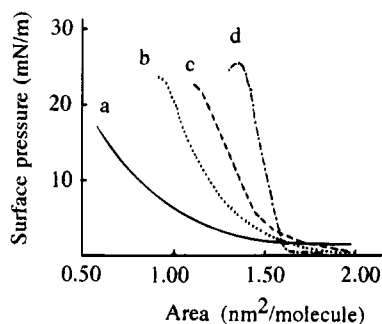
They ascribed the improved SHG signals to the molecular ordering and possible charge delocalization of the orderly segregated hemicyanine chromophore by the long alkyl chain of octadecylsulfate.

We also largely improved SHG signals by using several suitable rare earth complex anions as the counterions of the hemicyanine without the changes in charge transfer spectra. Therefore, the appreciable enlargements in  $\beta$  values for the complexes over  $A_{16}I$  are only due in part to the local field effect and may be primarily due to the molecular ordering and possible charge delocalization of hemicyanine chromophore when the hemicyanine cations were segregated by the bulky complex anions. This point of view was clearly demonstrated by the crystal structure of a model metal complex  $Me_2NC_6H_4CH=CHC_5H_4NC_2H_5La(TTA)_4$ . The crystal belongs to space group  $C2/c$ , with unit cell constants  $a = 2.7356(6)$ ,  $b = 1.0414(2)$ ,  $c = 2.4032(5)$  nm,  $\beta = 129.95(2)^\circ$ ,  $V = 5.249(5)$  nm<sup>3</sup>,  $Z = 4$ .<sup>36</sup> The packing diagram of the complex illustrated in Figure 2 is in accordance with that discussed above. The bulky lanthanide complex anion both separates and screens the chromophores of the hemicyanine, so, it is possible for the La complex to cause more charge delocalization in the hemicyanine and reduce inferior dipolar–dipolar interaction which usually cause centrosymmetric arrangement of the chromophores. This can also be indirectly supported by the work of Marder et al. dealing with the dependence of powder SHG signals on the counteranions of the hemicyanine.<sup>37</sup> It is noteworthy that the charge delocalization cannot simply be ruled out in the case of absence of spectral change, since the absence of spectral change may be due to the fact that the local inhomogeneity exceeds by far the dipolar coupling between neighboring chromophores.<sup>24</sup>

However, it should be emphasized again that the appreciable enlargements in  $\beta$  values is not general to all the lanthanide complexes, as seen from Table 1, and can be found in the lanthanide complexes which have substantially larger molecular areas and good film-forming properties. The effective charge separation in the hemicyanine by the lanthanide complexes could occur only for the complexes having good film-forming properties. The good film-forming properties seem an important prerequisite that the hemicyanine chromophores in the film are orderly segregated by the bulky lanthanide complex anions.

**TABLE 2: Influence of the Alkyl Chain Length of Complex  $A_nDy(PMBP)_4$  on the Film-Forming Properties and SHG**

materials	slope in collapse condense pressure region (mN/m)	molecular area (nm <sup>2</sup> )	$\chi^{(2)} \times 10^6$ (esu)	$\beta \times 10^{28}$ (esu)	$\phi$ (deg)	
$A_{16}I$	0.3	15.0	1.15	0.35–0.50	2.4–3.6	41.1
$A_{16}Dy(PMBP)_4$	1.08	24.7	1.84	0.59–0.87	6.6–9.8	29.1
$A_{12}Dy(PMBP)_4$	0.542	21.4	1.57	0.62–0.92	5.2–7.8	33.5
$A_4Dy(PMBP)_4$	0.606	22.4	1.34	0.19–0.29	6.2–9.3	36.5

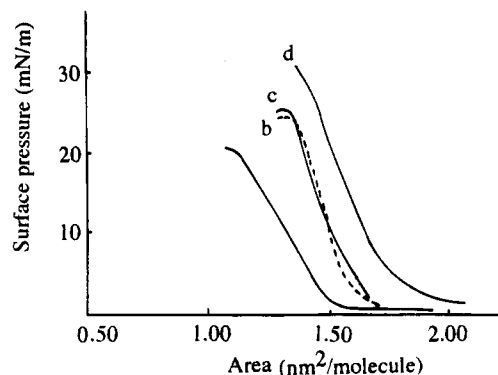
**Figure 3.** Influence of the alkyl chain length in  $A_nDy(PMBP)_4$  on film-forming properties: (a)  $A_{16}I$ ; (b)  $n = 4$ ; (c)  $n = 12$ ; (d)  $n = 16$ .

**Effect of Alkyl Chain Length of Hemicyanines on Film-Forming Properties and SHG.** The  $\pi$ - $A$  isotherms of three complexes with the composition of  $Me_2NC_6H_4CH=CHC_5H_4NC_nH_{2n+1}Dy(PMBP)_4$  ( $n = 16, 12,$  and  $4$ ), are shown in Figure 3. The slopes in the condensed regions of  $\pi$ - $A$  curves, collapse pressures, and molecular areas obtained from extrapolation of condensed region to a surface pressure of zero are given in Table 2. As can be seen from Figure 3 and Table 2, the three complexes have approximately the same molecular areas, indicating their having the same arrangement configuration within their Langmuir films despite their considerably different alkyl chain lengths. As for strongly hydrophilic  $A_{12}Br$  and  $A_4Br$ , they both cannot form a Langmuir film. The film formations, on the other hand, are gained when the bromide ions in these two compounds are replaced by the hydrophobic complex anion  $Dy(PMBP)_4$ . This breaks out of the traditional confinement of the film-forming materials to which the usually hydrophobic long alkyl chain has to be grafted.

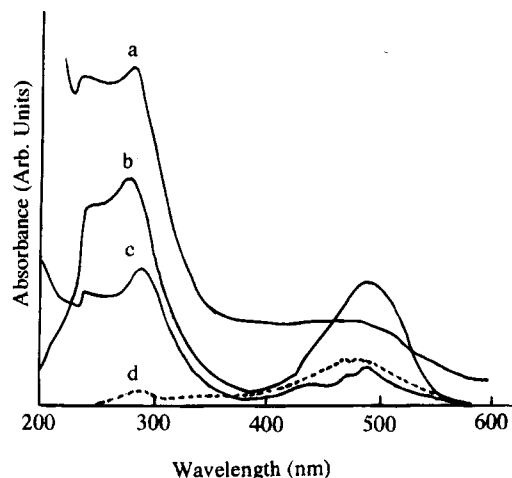
It is noteworthy that the tilt angle  $\phi$  of chromophores to the surface normal of the substrates decreases as the lanthanide complexes are formed. In the case of the same complex anion, the decreases of the angles may parallel to the improvement of film-forming properties, i.e., approximately proportional to the slopes in condensed regions. It can also be seen from Table 2 that the  $\beta$  values are not very sensitive to the variations of alkyl chain lengths.

**Influence of Central Ions in  $C_{16}Ln(PMBP)_4$  on Film-Forming Properties and SHG.** The  $\pi$ - $A$  isotherms for four complexes  $A_{16}Ln(PMBP)_4$  ( $Ln = La, Nd, Dy, Yb$ ) and  $A_{16}I$  are shown in Figure 4. The film-forming parameters and SHG results are given in Table 3. There is a tendency of a gradual increase in the slopes of condensed regions and collapse pressures as the ionic radius decreases ( $La^{3+} \rightarrow Yb^{3+}$ ); this is indicative of benefitting film formation as the central ions in the complexes change from light rare earth to heavy rare earth, although this improvement was not very large. However, the  $\beta$  values basically remain unchanged within error regions due to their similarity in ionic radii.

**Characterization of Homogeneity of Multilayer LB Films.** To demonstrate the homogeneity and ordered structure of the films, the complex  $A_{16}Dy(PMBP)_4$  was chosen to prepared the multilayer LB films. The absorption spectra of LB films and that of  $CHCl_3$  solution are compared in Figure 5. The ultraviolet

**Figure 4.** Influence of central ions in  $A_{16}Ln(PMBP)_4$  on film-forming properties: (a) La; (b) Nd; (c) Dy; (d) Yb.**TABLE 3: Effect of Central Ions in  $C_{16}X$  on Film-Formation and SHG**

counterion X	slope in condensed region	collapse pressure (mN/m)	molecular area (nm <sup>2</sup> )	$\chi^{(2)} \times 10^7$ (esu)	$\beta \times 10^{28}$ (esu)
$La(PMBP)_4$	0.56	21.2	1.50	5.5–7.9	5.5–8.1
$Nd(PMBP)_4$	0.86	24.1	1.65	5.5–8.1	6.1–9.1
$Dy(PMBP)_4$	1.08	24.7	1.68	5.9–8.7	6.6–9.8
$Yb(PMBP)_4$	0.96	28.9	1.75	5.8–8.6	6.8–10.1

**Figure 5.** UV-vis spectra: (a) 50-layer LB film of  $A_{16}Dy(PMBP)_4$ ; (b)  $A_{16}Dy(PMBP)_4$  in  $CHCl_3$ ; (c) monolayer film of  $A_{16}Dy(PMBP)_4$ ; (d) monolayer film of  $A_{16}I$ .

spectra of the films and the solution are very similar. The visible spectra, however, show some difference. The solution appears a well defined peaks at 490 nm. The 50-layer film of the complex, on the other hand, has a very broad absorption with no minimum in the visible, a slight shoulder at 490 nm. The monolayer of the complex exhibits a split peak with a maximum at approximately 492 nm, showing that the aggregations occur in the films. However, the monolayer film of  $A_{16}I$  has nearly same peak position (488 nm) as that of the complex. This indicates that the formation of the complex does not result in the large variation in the aggregation concentration in the films. The absorbances of the films at the wavelengths of 240 and 490 nm were measured as a function of the number of layers deposited and were found to be linearly dependent on the number of layers (Figure 6), indicating that the film is vertically uniform. Low angle X-ray diffraction diagrams for a 48-layer LB film on glass plate and 50 layers on  $CaF_2$  substrate are compared in Figure 7. A well-defined film structure was revealed by contrasting regular diffraction characteristics from LB films with polycrystalline pattern from powder sample. The LB film on glass substrate peaks at  $2\theta$  1.5, 2.96, and  $6.08^\circ$ ,

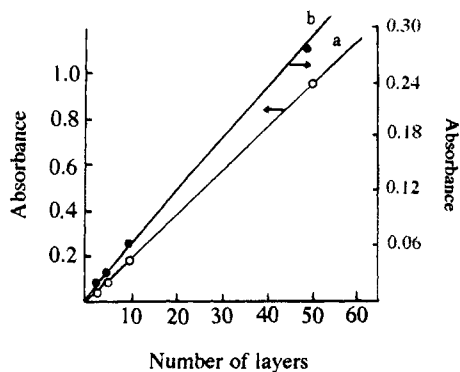


**Figure 6.** Absorbance change vs the number of layers of  $A_{16}Dy(PMBP)_4$ : (a) 240 nm; (b) 490 nm.

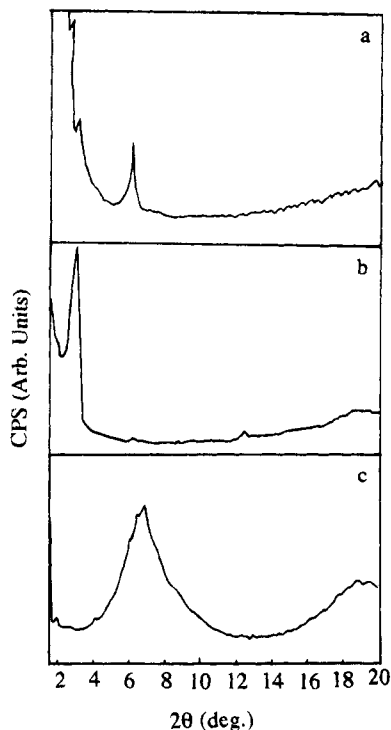


**Figure 7.** Low-angle X-ray diffraction diagrams: (a) the LB film (48 layers) on glass substrate; (b) the LB film (50 layers) on  $CaF_2$  substrate; (c) the powder complex  $A_{16}Dy(PMBP)_4$ .

which are assigned to (001), (002), and (004) Bragg diffraction, respectively. The average layer spacing of 58.8 Å was obtained according to the Bragg equation, and the single-layer film thickness 29.4 Å was thus derived. The LB film on  $CaF_2$  substrate peaks at  $2\theta$  3.08, 6.14 and 12.4°, which corresponds to (002), (004), and (008) Bragg diffraction, respectively. The obtained single layer film thickness of 28.6 Å agrees well with that from a glass substrate.

### Conclusion

The replacement of bromide and iodide counterions of hemicyanine by lanthanide complex anions is demonstrated to be a simple and successful method to improve Langmuir-forming and second harmonic generation properties. The values of second-order molecular hyperpolarizability  $\beta$  for lanthanide complexes with improved film-forming properties are largely enlarged compared with that for hemicyanine iodide. This is due in part to the local field effect but primarily the molecular ordering and ordered segregation of hemicyanine chromophore by the lanthanide complex anions, which was confirmed by low angle X-ray diffraction, the linear relationship of absorbance

vs the number of layers deposited, and the X-ray crystal structure of a model lanthanide complex.

**Acknowledgment.** The authors thank the National Climbing Plan and NNSFC for support of this project.

### References and Notes

- (1) Chemla, D. S.; Zyss, J. *Nonlinear Optical Properties of Organic Molecules and Crystal*; Chemla, D. S., Zyss, J., Eds.; Academic Press: Orlando, FL, 1987.
- (2) Zyss, J. *Non. Cryst. Solids* **1982**, *47*, 211.
- (3) Levine, B. F.; Bethea, C. G.; Thurmond, C. D.; Lynch, R. T.; Bernstein, J. L. *J. Appl. Phys.* **1979**, *50*, 2523.
- (4) Lipscomb, G. F.; Garito, A. F.; Narang, R. S. *J. Chem. Phys.* **1981**, *75*, 1509.
- (5) Williams, D. J. *Angew. Chem., Int. Ed. Engl.* **1984**, *23*, 690.
- (6) Marder, S. R.; Perry, J. W.; Schaefer, W. P. *Science* **1989**, *245*, 626.
- (7) Ashwell, G. J.; Hargreaves, R. C.; Baldwin, C. E.; Bahra, G. S.; Brown, C. R. *Nature* **1992**, *357*, 393.
- (8) Schildkraut, J. S.; Penner, T. L.; Willand, C. S.; Ulman, A. *Opt. Lett.* **1988**, *13*, 134.
- (9) Steinhoff, R.; Chi, L. F.; Marowsky, G.; Mobius, D. *J. Opt. Soc. Am.* **1989**, *B6*, 843.
- (10) Neal, D. B.; Petty, M. C.; Roberts, G. G. *J. Opt. Soc. Am.* **1987**, *B4*, 950.
- (11) (a) Wang, K. Z. Ph.D. Dissertation, Peking University, Beijing, 1993. (b) Zhou, D. J.; Huang, C. H.; Wang, K. Z.; Zhao, X. S.; Xie, X. M.; Xu, G. X.; Xu, L. G.; Li, T. K. *Langmuir* **1994**, *10*, 1910. (c) Li, H.; Huang, C. H.; Zhao, X. S.; Xie, X. M.; Xu, L. G.; Li, T. K. *Langmuir* **1994**, *10*, 3794.
- (12) Fendler, J. H. *Chem. Rev.* **1987**, *87*, 877.
- (13) Pomerantz, M. *Phase Transition in Surface Films*; Plenum: New York, 1980, p 9317.
- (14) Petty, M.; Lovett, D. R.; Oconnor, J. M. *Thin Solid Films* **1989**, *179*, 387.
- (15) (a) Wang, K. Z.; Huang, C. H.; Yao, G. Q.; Xu, G. X. *Chem. J. Chin. Univ. (China)* **1993**, *14*, 150. (b) Huang, C. H.; Wang, K. Z.; Zhu, X. Y.; Wu, N. Z.; Xu, G. X. *Solid State Commun.* **1994**, *90*, 151.
- (16) Choi, D. H.; Kim, N. M.; Wijekoon, W. M. K. P.; Prasad, P. N. *Chem. Mater.* **1992**, *4*, 1254.
- (17) Reid, J. C.; Calvin, M. *J. Am. Chem. Soc.* **1950**, *72*, 2948.
- (18) Dong, X. C.; Liu, F. C.; Zhao, Y. L. *Acta. Chim. Sin.* **1993**, *4*, 848.
- (19) Okafer, E. C. *Talanta* **1982**, *24*, 275.
- (20) Liu, L. Y.; Zhang, J. B.; Wang, W. C.; Zhang, Z. M.; Tao, F. G. *Opt. Commun.* **1992**, *93*, 207.
- (21) Zhang, T. G.; Zhang, C. H.; Wang, G. K. *J. Opt. Soc. Am.* **1990**, *B7*, 902.
- (22) Shen, Y. Q.; Shen, J. F.; Chiu, L.; Zhu, Z. Y.; Fu, X. F.; Xu, Y.; Liu, Y. Q.; Zhu, D. B.; Wang, W. C.; Liu, L. Y. *Thin Solid Films* **1992**, *208*, 280.
- (23) Cnossen, G.; Drabe, K. E.; Wiersma, D. A. *J. Chem. Phys.* **1992**, *97*, 4512.
- (24) Cnossen, G.; Drabe, K. E.; Wiersma, D. A.; Schoondorp, M. A.; Schouten, A. J.; Hulshof, J. B.; Feringa, B. L. *Langmuir* **1993**, *9*, 1974.
- (25) Ray, A.; Nag, K. *Bull. Chem. Soc. Jpn.* **1978**, *51*, 1525.
- (26) Okafor, E. C. *J. Inorg. Nucl. Chem.* **1980**, *42*, 1155.
- (27) Geary, W. J. *Coord. Chem. Rev.* **1971**, *7*, 81.
- (28) Marowsky, G.; Chi, L. F.; Mobius, D.; Steinhoff, R.; Shen, Y. R.; Dorsch, D.; Rieger, B. *Chem. Phys. Lett.* **1988**, *147*, 420.
- (29) Girling, I. R.; Cade, N. A.; Kolinsky, P. V.; Jones, R. J.; Peterson, I. R.; Ahmad, M. M.; Neal, D. B.; Petty, M. C.; Roberts, G. G.; Feast, W. J. *J. Opt. Soc. Am.* **1987**, *B4*, 950.
- (30) Scheelen, A.; Winant, P.; Persoons, A. *Conjugated Polymeric Materials: opportunities in Electronics and Molecular Electronics*; Bredas, J. L., Chance, R. R., Eds.; Kluwer Academic: Dordrecht, 1990; p 443.
- (31) Winant, P.; Scheelen, A.; Persoons, A. *Nonlinear Optical Effects in Organic Polymers*; Messier, J., Ed.; Kluwer Academic: Dordrecht, 1989; p 219.
- (32) Marowsky, G.; Steinhoff, R. *Opt. Lett.* **1988**, *13*, 707.
- (33) Shiota, K.; Kajikawa, K.; Takezoe, H.; Fukuda, A. *Jpn. J. Appl. Phys.* **1990**, *29*, 750.
- (34) Kajikawa, K.; Shiota, K.; Takezoe, H.; Fukuda, A. *Jpn. J. Appl. Phys.* **1990**, *29*, 913.
- (35) Kajikawa, K.; Takezoe, H.; Fukuda, A. *Jpn. J. Appl. Phys.* **1991**, *30*, 1050.
- (36) Wang, K. Z.; Huang, C. H.; Xu, G. X.; Wang, R. *J. Polyhedron*, in press.
- (37) Marder, S. R.; Perry, J. W.; Schaefer, W. P. *Science* **1989**, *245*, 626.